Full length article

Ferroelectric, upconversion emission and optical thermometric properties of color-controllable Er^{3+}-doped $Pb(Mg_{1/3}Nb_{2/3})O_3$-$PbTiO_3$-$Pb(Yb_{1/2}Nb_{1/2})O_3$ ferroelectrics

Teng Zheng, Laihui Luo*, Peng Du, Anmeng Deng, Weiping Li

Department of Microelectronic Science and Engineering, Ningbo University, 315211, Ningbo, China

ARTICLE INFO

ABSTRACT

The $(0.98-x)(0.6Pb(Mg_{1/3}Nb_{1/3})O_3-0.4PbTiO_3)$-$xPb(Yb_{1/3}Nb_{1/3})O_3$-$0.02Pb(Er_{1/2}Nb_{1/2})O_3$ $((0.98-x)(PMN-PT)$-$xPYN:Er^{3+})$ ceramics were prepared through a solid-state reaction method. The phase structure, piezoelectric response, ferroelectric performance and upconversion emission of the ceramics were systematically investigated. The phase structure, the electrical and optical properties are strongly related to the content of PYN. The optimized piezoelectric response and upconversion emissions of the ceramics were achieved near $x = 0.12$, which locates in the morphotropic phase boundary (MPB) composition. Furthermore, the temperature sensing behaviors of the resultant compounds based on the thermally coupled levels of $^2H_{11/2}$ and $^4S_{3/2}$ of Er^{3+} ions in the temperature range of 133–573 K were studied by utilizing the fluorescence intensity ratio technique. Additionally, the thermal effect, which is induced by the laser pump power, of the studied ceramics is also investigated and the produced temperature is enhanced from 268 to 348 K with the pump power rising from 109 to 607 mW.

1. Introduction

The lead based ferroelectric ceramics with general chemical formula of $Pb(B_1B_2)O_3$-$PTiO_3$ ($B_1 = Mg^{2+}$, Zn^{2+}, Yb^{3+}; $B_2 = W^{6+}$, Ta^{5+}, Nb^{5+} et al.), which possess superior piezoelectric and ferroelectric properties, have been extensively investigated [1–3]. Especially, the interest in the $(1-x)Pb(Mg_{1/3}Nb_{2/3})O_3$-$xPbTiO_3$ (PMN-PT) compounds with the composition near the morphotropic phase boundary (MPB) is increasing due to their high dielectric constant, admirable ferroelectric and piezoelectric performances [4,5]. Furthermore, the orthorhombic $P(Yb_{1/2}Nb_{2/3})O_3$ (PYN) at room temperature, as a member of the $Pb(B_1B_2)O_3$, has B-site cation disordering and a high Curie temperature of 302 °C [6]. Yoon et al. reported that the ferroelectric properties of the $Pb(Zr_{0.52}Ti_{0.48})O_3$ ceramics were greatly enhanced with the introduction of the PYN [7]. In our previous work, we also found that the PYN exhibited a distinct effect on the ferroelectric and dielectric behaviors of the $PbTiO_3$ ceramics [8]. It seems that the addition of PYN into other ceramic hosts is an efficient method to improve their ferroelectric and piezoelectric properties. Unfortunately, to the best of our knowledge, the investigation on the effect of PYN on the ferroelectric and piezoelectric properties of PMN-PT ceramics has not been carried out. Therefore, it would be very necessary to analyze the influence of PYN on the ferroelectric and piezoelectric properties of PMN-PT ceramics.

On the other hand, the trivalent rare-earth (RE) ions doped upconverting materials, which possess outstanding advantages of sharp emission band, absence of auto-fluorescence, large anti-Stokes shift and long luminescence lifetime, have attracted considerable attention due to their potential applications in cell imaging, optical thermometry, solar cell and solid state lighting [9–13]. Among these RE ions, the Er^{3+} ion is considered as a promising candidate for upconverting materials as activator because of its unique upconversion (UC) emissions originating from the intra-4f transitions [14,15]. However, the Er^{3+} ion usually possesses low absorption in the near-infrared region, leading to low luminescent efficiency in Er^{3+} ions single doped upconverting materials. To figure out this shortage, the Yb^{3+} ion, which acts as the sensitizer, is introduced on account of its large absorption cross section in the near-infrared region as well as the proper energy overlap between the Yb^{3+} and Er^{3+} ion, resulting in the efficient energy transfer (ET) from Yb^{3+} to Er^{3+} ions and enhancing the UC emission performances of the Er^{3+} ions [16,17]. Song et al. revealed that the $LiYF_4$:Er^{3+}/Yb^{3+} upconverting nanocrystal can exhibit highly efficient UC emissions and were suitable for photovoltaic devices [18]. Furthermore, Hao et al. reported that the $NaYbF_4$:Er^{3+} nanoparticles, which can emit bright red UC emissions, had potential applications in *in vivo* bioimaging [19]. In

comparison with other inorganic materials, ferroelectric ceramics are multifunctional materials in which the ferroelectric, piezoelectric, dielectric and pyroelectric properties can be simultaneously realized. Currently, researchers have revealed that the ferroelectric ceramics can exhibit enhanced ferroelectric, piezoelectric and satisfactory photoluminescence properties with the introduction of RE ions [20–23]. Chu et al., pointed out the ferroelectric and dielectric properties of the $Na_{0.5}Bi_{4.5}Ti_4O_{15}$ piezoelectric ceramics were greatly enhanced after doping the Er^{3+} ions [24]. Kwok et al. disclosed that the $0.93Bi_{0.5}Na_{0.5}TiO_3$-$0.07BaTiO_3$:$Er^{3+}$ ceramics did not only exhibit bright UC emission but also possess admirable ferroelectric properties [25]. Similar results were also observed in other RE ions doped ceramics, such as PMN-PT:Er^{3+}, $CaBi_4Ti_4O_{15}$:Ho^{3+}, $0.94Bi_{0.5}Na_{0.5}TiO_3$-$0.06BaTiO_3$/ZnO:$Er^{3+}$ and $PbZr_{0.52}Ti_{0.48}O_3$:Er^{3+} [26–29]. Although many efforts have been made and some impressive achievements have been obtained, as far as we know, the reports on the ferroelectric, piezoelectric and UC emission behaviors of Er^{3+} ions doped PMN-PT-PYN have not been reported. Therefore, in present work, we designed a new solid solution formed from tetragonal $0.6Pb(Mg_{1/3}Nb_{1/3})O_3$-$0.4PbTiO_3$ and the orthorhombic PYN to achieve high piezoelectric response near MPB. To obtain possible UC emission, a content of 2 mol % Er^{3+} was doped in the designed compound. Namely, $(0.98-x)(0.6Pb(Mg_{1/3}Nb_{1/3})O_3$-$0.4PbTiO_3)$-$xPb(Yb_{1/3}Nb_{1/3})O_3$-$0.02Pb(Er_{1/2}Nb_{1/2})O_3$ $((0.98-x)(PMN-PT)$-$xPYN$:$Er^{3+})$ ceramics were prepared by means of a traditional solid-state reaction method. The phase composition, microstructure, luminescent mechanism, ferroelectric, piezoelectric and UC emission properties of the final products were systematically analyzed. With the help of the fluorescence intensity ratio (FIR), the optical thermometric behaviors of the studied samples were investigated. Ultimately, the internal heating properties caused by the excitation pump power of the resultant compounds were also studied to explore its feasibility for optical heater.

2. Experimental

The $(0.98-x)(PMN-PT)$-$xPYN$:Er^{3+} (x = 0.00, 0.06, 0.10, 0.12, 0.14 and 0.16) ceramics were synthesized by means of a two-stage sintering route [26]. The high purity powders of PbO (99.99%), MgO (99.9%), Er_2O_3 (99.9%), Nb_2O_5 (99.5%), Yb_2O_3 (99.9%) and TiO_2 (99.8%), which were purchased from Aladdin, were used as the raw materials. Briefly, to prepare the PYN compounds, the $Yb_{1/2}Nb_{1/2}O_2$ should be firstly synthesized. The stoichiometric ratio of Yb_2O_3 and Nb_2O_5 were weighted and ball-milled with alcohol for 12 h. Then, the slurry was dried and calcined at 1200 °C for 1 h to achieve the $Yb_{1/2}Nb_{1/2}O_2$ cake. After that, the $Yb_{1/2}Nb_{1/2}O_2$ was crushed by ball-milling. Subsequently, the PbO was added to the $Yb_{1/2}Nb_{1/2}O_2$ and mixed powders of PbO and $Yb_{1/2}Nb_{1/2}O_2$ were shifted to furnace and sintered at 830 °C for 2 h to generate the PYN.

Afterwards, the stoichiometric ratio of MgO (excess 5 mol%) and Nb_2O_5 were weighted and ball-milled with alcohol for 12 h. Then, the slurry was dried and calcined at 1100 °C for 4 h to synthesize $MgNb_2O_6$. According to the chemical formula of PMN-PT, the crushed $MgNb_2O_6$, PbO (excess 3 mol%) and TiO_2 were weighted and totally mixed with each other. The slurry was then dried and pre-sintered at 885 °C for 2 h to synthesize the perovskite PMN-PT. Finally, on the basis of the chemical formula of $(0.98-x)(PMN-PT)$-$xPYN$:Er^{3+}, the stoichiometric ratio of PbO and Er_2O_3 were added into the mixture of PYN and PMN-PT powders and mixed in alcohol by agate ball for 12 h. After that, the slurry was dried and pre-sintered at 850 °C for 2 h. Subsequently, they were remilled and thorough mixed with poluvinyl alcohol binder solution and pressed into pellets. Finally these pellets were sintered at 1180 °C for 2 h in air and the $(0.98-x)(PMN-PT)$-$xPYN$:Er^{3+} ceramics were successfully synthesized.

The phase structure of the ceramics was evaluated using an X-ray diffractometer (D8 Advance, Bruker AXS, Karlsruhe, Germany) with Cu Kα radiation. Polarization *vs.* electric field (*P-E*) hysteresis loops were

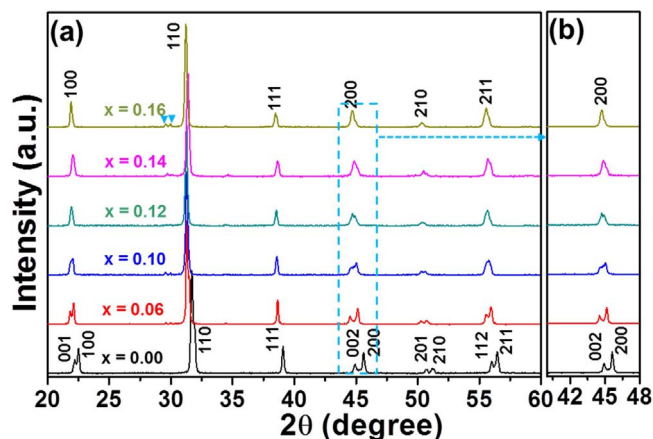**Fig. 1.** (a) XRD patterns of $(0.98-x)(PMN-PT)$-$xPYN$:Er^{3+} ceramics. (b) Zoomed XRD patterns from 40 to 48°.

recorded at 1 Hz with the help of a RT Premier II ferroelectric workstation. The ceramics were poled under an electric field of 2 kV/mm at room temperature. The piezoelectric coefficient d_{33} of studied samples was measured using a quasistatic piezoelectric meter (ZJ-3AN, China). Dielectric constants ε_{33} were measured at 1 kHz utilizing an impedance analyzer (Agilent 4294A). The scanning electron microscope (SEM) (Hitachi SU-700) was used to examine the morphological properties of the studied compounds. The UC emission spectra of the resultant ceramics were detected by a spectrofluormeter (Edinburgh FS5) equipped with a pump power controllable 980 nm laser diode (ADR-1805). The temperature ranging from 133 to 573 K was modulated by utilizing the temperature controlled system (Linkam HFS600E-PB2).

3. Results and discussion

The phase purity and crystal structure of the synthesized ceramics were identified by means of the X-ray diffraction (XRD) analyzer. The XRD patterns of the $(0.98-x)(PMN-PT)$-$xPYN$:Er^{3+} ceramics with various PYN contents were measured and depicted in Fig. 1(a). A pure perovskite structure of PMN-PT is obtained, and a trace of pyrochlore phase as marked in the figure is detected as PYN is introduced. As presented, when x = 0.00, two significant peaks of (002) and (200), which are assigned to the characteristic peaks of tetragonal phase, are observed. However, with the increase of the PYN content, these two peaks become closer and closer, and become very obscure when x is increased to 0.10, as presented in Fig. 1(b). Meanwhile, when the PYN content is increased to x = 0.12, the (002) and (200) peaks are vanished and merged into a broad diffraction peak of (200) corresponding to a MPB phase. With further raising the PYN content to x = 0.14, this broad (200) peak becomes sharp, implying that the resultant compounds transform into a pseudocubic phase. This XRD result demonstrates that the phase of the prepared ceramics is tetragonal at $x \leq 0.06$, MPB phase $0.10 \leq x \leq 0.14$, and finally transit to pseudocubic phase with $x \geq 0.16$. To examine the influence of PYN content on the microstructure of the prepared samples, the representative SEM images of the polished cross-sections for $(0.98-x)(PMN-PT)$-$xPYN$:Er^{3+} (x = 0.00, 0.10, 0.14 and 0.16) ceramics after thermal etching at 1000 °C for 2 h were demonstrated in Fig. 2. The SEM images shown in Fig. 2 reveal that all the ceramics are densely sintered without detecting significant pores. The calculated density of these $(0.98-x)(PMN-PT)$-$xPYN$:Er^{3+} ceramics for x = 0.00, 0.06, 0.10, 0.12, 0.14 and 0.16 are 92.6%, 91.3%, 95.8%, 92.7%, 91.2%, 93.4%, respectively. Furthermore, the resultant prepared ceramics are composed of inhomogeneous grains with the particle size ranging from approximately 2–15 μm. Note that, with the introduction of the PYN, the shape of the $(0.98-x)(PMN-PT)$-$xPYN$:Er^{3+} grains becomes more irregular (see Fig. 2(a) and (b)),